Structure-property relationships in azobenzene-based twist-bend nematogens

Jordan P Abberley, John MD Storey and Corrie T Imrie*

Department of Chemistry, School of Natural and Computing Sciences, University of Aberdeen, Meston Building, Old Aberdeen AB24 3UE, UK

*Author for correspondence; email c.t.imrie@abdn.ac.uk

1

Abstract

The synthesis and characterisation of a new set of azobenzene-based non-symmetric liquid crystal dimers, the 1-(4-substitutedazobenzene-4'-yloxy)-6-(4-methoxybiphenyl-4'-yl)hexanes (MeOB6OABX), that exhibit the twist-bend nematic phase, N_{TB}, is described. The terminal substituents are methyl, methoxy, ethyl, butyl, butoxy, and nitrile. All six dimers exhibit both the N_{TB} and conventional nematic, N, phases. The identification of the N_{TB} phase was performed using polarised light microscopy and confirmed for binary mixtures with a standard twist-bend nematogen 1,7-bis-4-(4'-cyanobiphenyl) heptane (CB7CB). The transitional behaviour of the MeOB6OABX dimers is compared with that of the corresponding ether-linked 1-(4-substitutedazobenzene-4'-yloxy)-6-(4-methoxybiphenyl-4'-yloxy)pentanes, MeOBO5OABX, all of which exhibit a conventional nematic phase. In addition, the nitrile-substituted MeOBO5OABCN shows the N_{TB} phase. The behaviour of these nonsymmetric dimers is also compared to that of the corresponding symmetric dimers. Differences in the transitional properties between these sets of new materials are accounted for in terms of not only molecular shape but also other factors including the strength of the mixed mesogen interaction.

Introduction

The twist-bend nematic (N_{TB}) phase is fascinating for many reasons but not least for the observation of spontaneous chirality in a system consisting of achiral molecules [1]. In the N_{TB} phase, the director forms a conical helix in which it is tilted with respect to the helical axis, with doubly degenerate domains of opposite handedness. Meyer first predicted the N_{TB} phase for a system consisting of polar molecules in which interactions between the particles induced bend deformations [2]. Almost twenty years later and independently, Dozov predicted the existence of the N_{TB} phase using a model based on the proposal that bent molecules have a natural tendency to pack into bent structures [3]. However, pure uniform bend in space is not allowed and so the director bend must be accompanied by other local deformations of the director, namely, twist or splay, giving rise to the twist-bend or splay-bend nematic phase, respectively. Thus in Dozov's model it is the bent shape of the molecules that drives the formation of the N_{TB} phase and this is accounted for in terms of anomalously low bend elastic constants in such systems [3].

A decade after Dozov's seminal paper [3], the N_{TB} phase was discovered by Cestari *et al* for 1,7-bis-4-(4'-cyanobiphenyl) heptane, CB7CB [4],
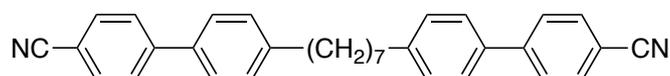
and the assignment confirmed initially using freeze fracture transmission electron microscopy [5, 6] and more recently by resonant X-ray scattering [7]. The helical pitch length in the N_{TB} phase was found to be strikingly small, typically around 10 nm, which corresponds to just 3-4 molecular distances [5-7]. Although Cestari *et al* reported the first unambiguous identification of the N_{TB} phase [4], there exist earlier accounts of nematic-nematic transitions which, with hindsight, are nematic (N) – N_{TB} transitions (see, for example, [8, 9]). Dozov, as part of the same work, also predicted the formation of heliconical smectic phases by systems consisting of achiral bent molecules and these have recently also been discovered [10, 11].

CB7CB [4] and, indeed, the other early examples of twist-bend nematogens [8, 9] belong to a class of mesogenic materials known as liquid crystal dimers that consist of molecules containing two mesogenic groups

attached through a flexible spacer, most commonly an alkyl chain [12, 13]. The transitional properties of liquid crystal dimers are strongly dependent on the length and parity of the spacer, and in a manner strongly reminiscent of the behaviour of semi-flexible main–chain liquid crystal polymers. Indeed, the early interest in this class of low molar mass liquid crystals stemmed from their potential to serve as model compounds not only for main-chain [14] but also for side-chain liquid crystal polymers [15]. It soon became apparent, however, that liquid crystal dimers were of significant fundamental interest in their own right and proved to be a rich vein for the discovery of new types of smectic phases, most notably intercalated phases [16-19]. The pronounced alternation in the transitional properties of a homologous series of dimers observed on varying the parity of the spacer is most often accounted for in terms of the different shapes of the molecules having odd or even membered spacers and their associated conformational distributions [13]. Specifically, dimers containing an even-membered spacer are, on average, linear whereas those with an odd-membered spacer are bent. Furthermore, the nature of the link between the spacer and mesogenic units plays a critical role in determining the extent of the molecular curvature, and methylene-linked dimers are more strongly bent than their ether-linked counterparts [20, 21].

There are now a relatively large, and growing, number of twist-bend nematogens reported in the literature, the majority of which are odd-membered methylene-linked liquid crystal dimers (see, for example, [22-28]) although other linkages have been used (see, for example, [29-42]). Other types of structure known to exhibit the N_{TB} phase include semi-flexible bent core liquid crystals [43, 44], higher oligomers [45-49] and hydrogen-bonded structures [50-52]. The common structural feature connecting these various materials is a bent molecular shape and this appears to be a prerequisite for the observation of the N_{TB} phase. [29, 41, 53-56]. These bent molecular shapes also give rise to conventional nematic phases having anomalously low bend elastic constants [5, 57, 58] and such materials may be exploited in new applications [59-62]. The N_{TB} phase is normally preceded by a conventional N phase but this is not always the case and direct N_{TB}-I transitions have been observed for dimers having short

odd-membered spacers [34, 35] and also for a dimer doped with a highly chiral compound [63].

Although a relatively large number of twist-bend nematogens have now been reported, we are still at an early stage of establishing and understanding structure-property relationships in this class of materials. We have recently reported the transitional behaviour of the 1-(4-substitutedazobenzene-4'-yloxy)-6-(4-cyanobiphenyl-4'-yl)hexanes [64],

NC—⟨benzene⟩—⟨benzene⟩—(CH$_2$)$_6$O—⟨benzene⟩—N=N—⟨benzene⟩—X

X = Me, OMe, Bu, OBu, CN, NO$_2$
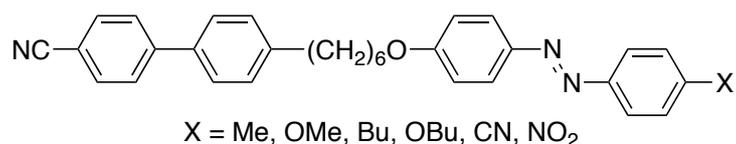
and referred to them using the acronym CB6OABX in which CB and AB refer to the cyanobiphenyl and azobenzene moieties, respectively, and 6O the hexyloxy spacer. All six dimers exhibited the N_{TB} phase and there appeared to be no simple correlation between the electronic properties of the mesogenic units and the formation of the N_{TB} phase. In order to extend this study and better understand the relationships between structure and the formation of the N_{TB} phase, here we report the synthesis and characterisation of the closely structurally related 1-(4-substitutedazobenzene-4'-yloxy)-6-(4-methoxybiphenyl-4'-yl)hexanes,

MeO—⟨benzene⟩—⟨benzene⟩—(CH$_2$)$_6$O—⟨benzene⟩—N=N—⟨benzene⟩—X

X = Me, OMe, Et, Bu, OBu, CN
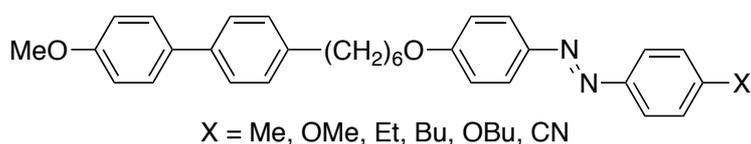
and by analogy described these dimers using the acronym MeOB6OABX in which MeOB denotes methoxy biphenyl. We have focussed on this structure because azobenzene-based liquid crystals are an important class of photoresponsive materials [65-68]. Indeed, we have shown that for CB6OABOBu an isothermal, reversible N_{TB}-N transition may be driven photolytically [69-71]. Such investigations, however, are outwith the scope of the present study which is focussed solely on establishing and understanding structure-property relationships for this set of dimers. In order to achieve this goal, we compare the properties of the MeOB6OABX dimers to those of the corresponding dimers in which the methylene link has been replaced by an ether link, the 1-(4-substitutedazobenzene-4'-yloxy)-6-(4-methoxybiphenyl-4'-yloxy)pentanes, MeOBO5OABX,

X = Me, OMe, Et, Bu, OBu, CN
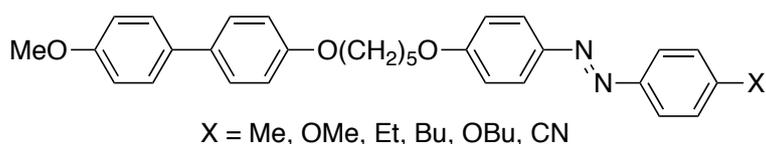
The transitional properties of these two sets of nonsymmetric dimers are further compared to those of the corresponding symmetric dimers, the 1,5-bis(4-substitutedazobenzene-4'-yloxy)pentanes, XABO5OABX, [64]


X = Me, OMe, Et, Bu, OBu, CN

,
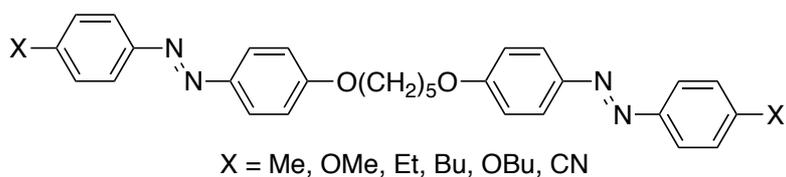
CB7CB [4, 36] and 1,7-bis(4-methoxybihenyl-4'-yl)heptane, MeOB7BOMe

.
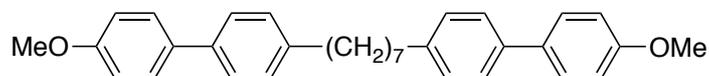
Experimental

Synthesis

The synthetic routes used to obtain the MeOB6OABX and MeOBO5OABX dimers are shown in Scheme 1. The synthesis and characterisation of the XABO5OABX dimers have been reported previously [64] with the exception of EtABO5OABEt which was prepared by the reaction of 4-hydroxy-4'-ethylazobenzene with 1,5-dibromopentane. The syntheses of 4'-hydroxy-4-methoxybiphenyl (**4**), 1-{4-[(5-bromopentyl)oxy]phenyl}-4-methoxybenzene (**5**) [72] and the 4-hydroxy-4'-substitutedazobenzenes (**3**) have been described elsewhere [73-77]. Full synthetic descriptions and structural characterisation data for all the final products and new intermediates are given in the associated supplementary information.
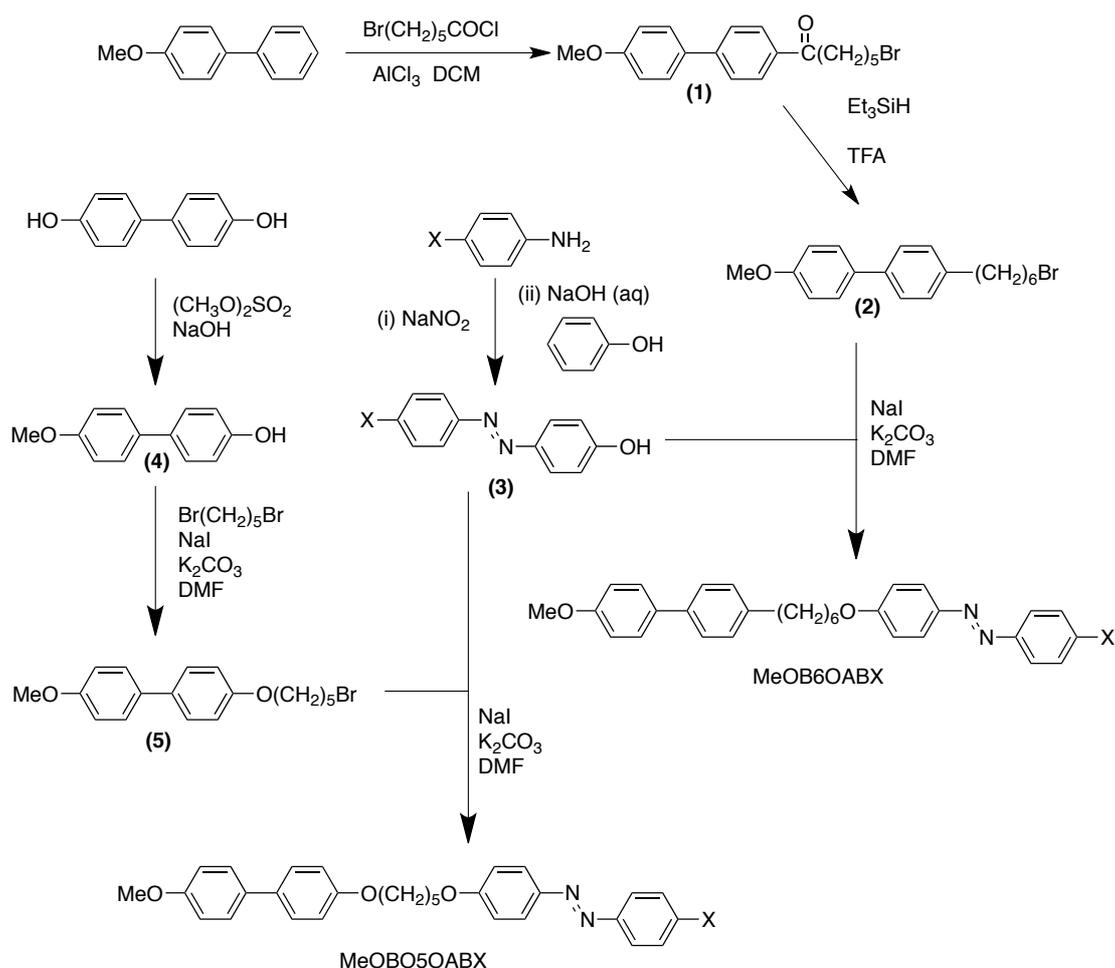
Scheme 1. Syntheses of the MeOB6OABX and MeOBO5OABX dimers.

Phase Diagrams

To confirm phase assignments a number of phase diagrams were constructed. Binary mixtures of selected dimers were prepared by codissolving preweighed amounts of the appropriate dimers in dichloromethane and the solvent allowed to slowly evaporate at room temperature. Each mixture was further dried under vacuum at 50 °C overnight.

Thermal Characterisation

The phase behaviour of the dimers and their mixtures was studied by differential scanning calorimetry using a Mettler-Toledo DSC820 fitted with an intracooler and calibrated using indium and zinc as standards. Heating and cooling rates were 10 °C min^{-1} and all samples were measured under a nitrogen atmosphere. Transition temperatures and associated enthalpy changes were extracted from

the second heating trace unless otherwise noted. For each sample, two aliquots were measured and the data listed are the average of the two sets of data. Phase assignments were made using polarised light microscopy using an Olympus BH2 microscope equipped with a Linkam TMHS 600 heating stage. All the microscopy studies of the azobenzene-based materials were performed using a 50.8 mm square longpass filter with a 495 nm cut-off (Edmund Optics) in order to prevent the photoisomerisation of the azobenzene moiety.

Molecular Modelling

The geometric parameters and electronic properties of the dimers were calculated using quantum mechanical density functional theory [78]. Geometric optimisation of the dimers with the spacer in the all-*trans* conformation was performed using Gaussian G09W at the B3LYP/6-31G(d) level of theory. The all-*trans* conformers were exclusively selected for reasons to be discussed later. Visualisation of space-filling models of the output post-optimisation was performed using QuteMol [79], and Gaussview 5 was used for the visualisation of electrostatic potential isosurfaces, ball-and-stick models and dipole moments [80].

Results and Discussion

MeOB6OABX dimers

The transitional properties of the MeOB6OABX dimers are listed in Table 1. All the dimers exhibit a monotropic conventional nematic (N) phase with the exception of MeOB6OABCN for which an enantiotropic N phase is observed. Throughout this study conventional N phases have been assigned on the basis of the observation of a characteristic Schlieren optical texture containing both two and four brush point singularities when viewed through the polarising light microscope, and which flashed when subjected to mechanical stress. A representative nematic Schlieren optical texture is shown as Figure 1(a). The associated entropy changes are wholly consistent with these nematic-isotropic assignments [38, 64]. On cooling the higher temperature N phase of MeOB6OABCN, a blocky texture developed characteristic of the N_{TB} phase, see

Figure 1(b). In addition, the N-N_{TB} transition was accompanied by the cessation of the optical flickering associated with the fluctuations of the director in the conventional nematic phase. The entropy change associated with the N-N_{TB} transition is small and consistent with the relatively long temperature range of the conventional N phase [36]. Bulk samples of the N phases of the remaining MeOB6OABX dimers simply crystallised on cooling. It was possible, however, to supercool isolated drops of each dimer to lower temperatures and the Schlieren nematic texture changed to give a combination of focal conic fans and rope-like textures characteristic of the N_{TB} phase. These transitions were also accompanied by the cessation of the optical flickering characteristic of the higher temperature conventional N phase. The monotropic nature of the twist-bend nematic phases precluded their study using X-ray diffraction and so the phase assignments were confirmed by miscibility studies. For these studies CB7CB [4, 36] was chosen as the standard twist-bend nematogen. For example, Figure 2 shows the phase diagram constructed for binary mixtures of MeOB6OABOMe and CB7CB, and complete miscibility is observed between the two dimers over the entire compositional range. Each binary mixture exhibited N_{TB} and N phases, and these were characterised on the basis of the observation of characteristic optical textures. In addition, the N_{TB}-N transition temperature ($T_{N_{TB}N}$) measured for supercooled isolated drops of MeOB6OABOMe is in excellent agreement with the extrapolated value based on the transition temperatures observed for the mixtures. On increasing the amount of MeOB6OABOMe in the mixtures, T_{NI} increases in essentially a linear manner. By comparison, $T_{N_{TB}N}$ decreases and the N_{TB}-N phase boundary shows a small but consistent positive deviation from linear behaviour. Similar behaviour is seen in Figure 3 for the phase diagram of binary mixtures of MeOB6OABEt and CB7CB although the much lower T_{NI} of MeOB6OABEt compared to MeOB6OABOMe gives an increasing linear N-I phase boundary. Within the framework of a molecular field theory developed to predict phase diagrams for binary mixtures of nematics [81], the linear dependence of T_{NI} on composition seen in both Figures 2 and 3 suggests that the intermolecular energy parameter between the unlike species is the geometric mean of the interaction parameters between the like species. It would be

tempting to account for the upward curvature seen for the $T_{N_{TB}N}$ line in Figures 2 and 3 in terms of a specific interaction between the unlike mesogenic groups [17]. However, such an interaction would normally give rise to a concurrent upward curvature in the T_{NI} line and this is not observed. Instead, it has been suggested that the difference in shapes between the two components may be at the root of the enhanced N_{TB} behaviour seen in mixtures such as these [36]. Specifically, the transitional properties of methylene- and ether-linked dimers may be understood in terms of the bond angle between the *para* axis of the mesogenic unit and the first bond in the spacer [82-84]. For methylene-linked dimers this bond angle is 113.5° and for an ether link 126.4°. This larger bond angle for the ether-link gives a more linear structure than for a methylene link. The upward curvature of the $T_{N_{TB}N}$ line may be associated with an enhanced ability of the molecules in the mixtures to pack into a locally intercalated arrangement facilitated by the more linear ether-linked fragment. Such an intercalated packing arrangement is commonly observed in both the N_{TB} and preceding N phases [36] although the physical significance of this observation in terms of the stabilisation the N_{TB} phase has recently been questioned [55].

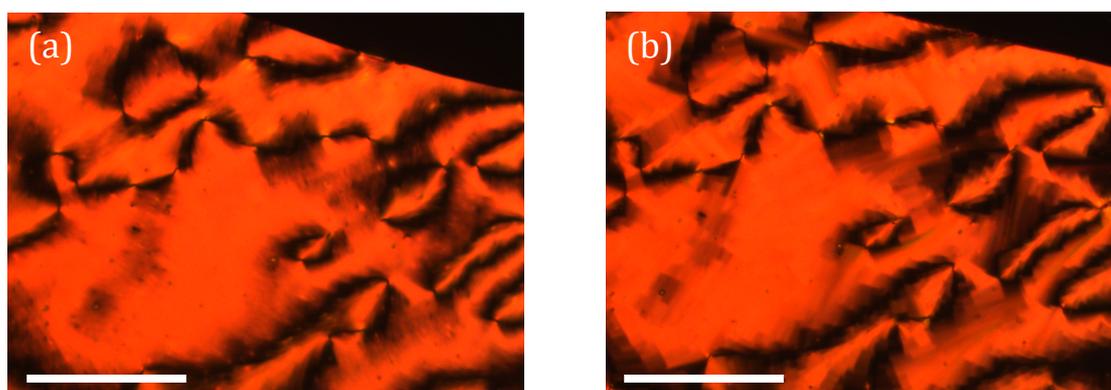**Figure 1.**   (a) The Schlieren texture of the nematic phase (T=109 °C), and (b) the blocky texture of the twist-bend nematic phase (T=106 °C) for MeOB6OABCN. The textures are of approximately the same region of the slide. The scale bars represent 50 μm.

Table 1. Transitional properties of the MeOB6OABX dimers. (Cr, crystal; N_{TB}, twist-bend nematic; N, nematic; I, isotropic).

X	T_{CrI}/°C [a]T_{CrN}/°C	$T_{N_{TB}N}$/°C	T_{NI}/°C	ΔH_{CrI} [a]ΔH_{CrN} /kJ mol^{-1}	*ΔH_{NI} /kJ mol^{-1}	ΔS_{NI}/R
Me	131.2	73.4	122.5	45.86	0.81	0.25
MeO	154.3	94.9	151.1	65.00	1.22	0.35
Et	119.4	66.9	112.1	42.75	0.54	0.17
Bu	111.9	71.3	109.0	46.16	0.62	0.20
BuO	148.1	93.6	140.8	55.61	0.88	0.26
CN	[a]132.3	[b]107.7	159.9	[a]47.19	0.94	0.26

*Exotherms associated with the N-I transition have been measured on cooling with the exception of that for MeOB6OABCN. The corresponding transition temperatures have been measured on heating using the polarising light microscope.

[b]$\Delta H_{N_{TB}N}$=0.15 kJ mol^{-1}; $\Delta S_{N_{TB}N}$/R=0.05.

Figure 2. Phase diagram constructed for binary mixtures of CB7CB and MeOB6OABOMe. Triangles represent N-I transition temperatures and squares twist-bend nematic-nematic transition temperatures. The broken line connects the melting points.
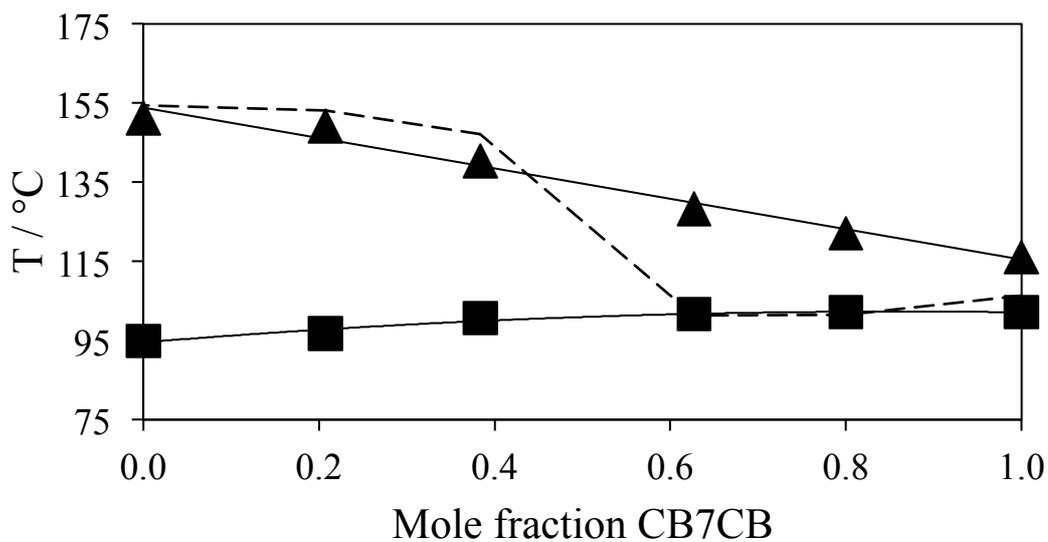

Figure 3. Phase diagram constructed for binary mixtures of CB7CB and MeOB6OABEt. Triangles represent N-I transition temperatures and squares twist-bend nematic-nematic transition temperatures. The broken line connects the melting points.
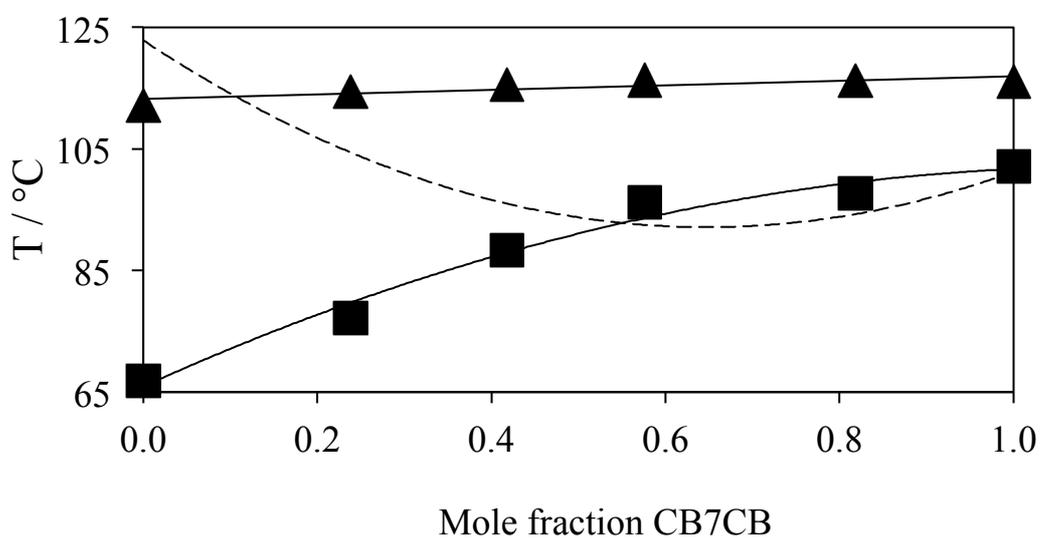
MeOBO5OABX dimers

The transitional properties of the MeOBO5OABX dimers are listed in Table 2. MeOBO5OABOMe and MeOBO5OABCN exhibit enantiotropic nematic phases and the remaining dimers are monotropic nematogens. The nematic phases were identified on the basis of the characteristic Schlieren textures observed as described earlier. The entropy changes associated with these N-I transitions are wholly consistent with this phase assignment [85, 86]. On cooling isolated droplets of MeOBO5OABCN, the Schlieren nematic texture changed to give a fan-like texture suggesting a strongly monotropic twist-bend nematic phase, see Figure 4. To confirm this assignment a phase diagram was constructed for binary mixtures of MeOBO5OABCN and CB7CB, see Figure 5. All the binary mixtures exhibited a higher temperature conventional N phase and on cooling, an N_{TB} phase. The optical textures observed for the 60 mol% mixture of MeOBO5OABCN with CB7CB are shown in Figure 6. Complete miscibility was observed for the N and N_{TB} phase across the whole composition range. In addition, the $T_{N_{TB}N}$ measured for supercooled isolated drops of MeOBO5OABCN is in excellent agreement with the extrapolated value based on the transition temperatures observed for the mixtures. The T_{NI} and $T_{N_{TB}N}$ lines both show an upward curvature unlike the behaviour seen in Figures 2 and 3. This suggests that the intermolecular energy parameter between the unlike species in this mixture is greater than the geometric mean of the interaction parameters between the like species [81].

Table 2. Transitional properties of the MeOBO5OABX dimers. (Cr, crystal; N_{TB}, twist-bend nematic; N, nematic; I, isotropic).

X	T_{CrI}/°C $^aT_{CrN}$/°C	$T_{N_{TB}N}$/°C	T_{NI}/°C	ΔH_{CrI} $^a\Delta H_{CrN}$ /kJ mol^{-1}	$^*\Delta H_{NI}$ /kJ mol^{-1}	ΔS_{NI}/R
Me	169.4		159.7	70.63	1.56	0.44
MeO	^{a}186.5		188.3	^{a}77.66	2.18	0.57
Et	160.4		150.4	56.03	^{b}-	-
Bu	150.9		146.4	60.98	1.12	0.32
BuO	179.8		171.2	76.38	1.78	0.48
CN	^{a}180.1	91.6	192.4	^{a}62.92	1.62	0.42

*Exotherms associated with the N-I transition have been measured on cooling with the exception of that for MeOBO5OABCN. The corresponding transition temperatures have been measured on heating using the polarising light microscope. [b]Crystallisation precluded the measurement of the enthalpy change associated with the N-I transition for MeOBO5OABEt.
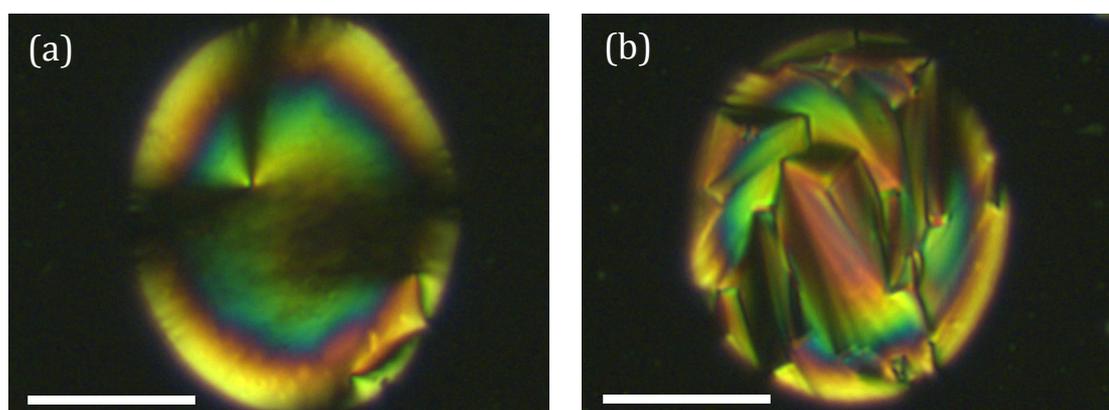

Figure 4. (a) The Schlieren texture of the nematic phase (T=99 °C), and (b) the fan texture of the twist-bend nematic phase (T=88 °C) for MeOBO5OABCN. The textures are of approximately the same region of the slide. The scale bars represent 50 μm.
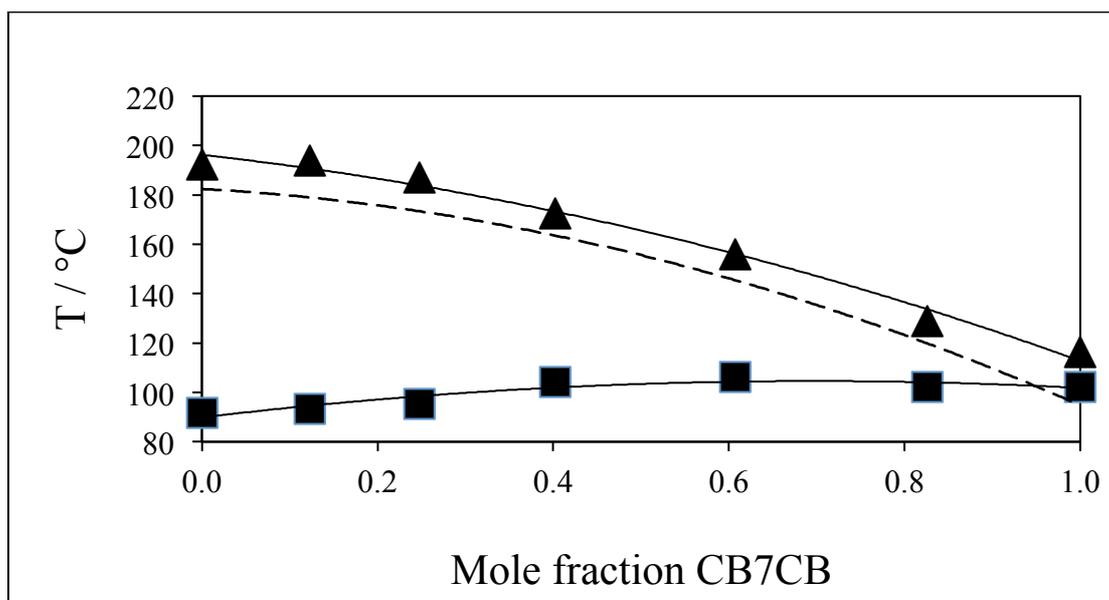
Figure 5. Phase diagram constructed for binary mixtures of CB7CB and MeOBO5OABCN. Triangles represent N-I transition temperatures and squares twist-bend nematic-nematic transition temperatures. The broken line connects the melting points.
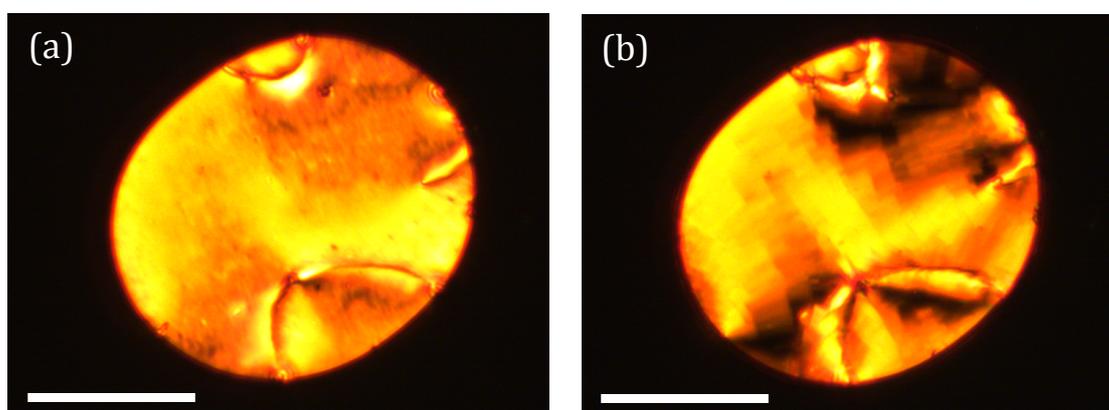
Figure 6. (a) The Schlieren texture of the nematic phase (T=109 °C), and (b) the blocky texture of the twist-bend nematic phase (T=103 °C) for a 60 mol% mixture of MeOBO5OABCN with CB7CB. The textures are of approximately the same region of the slide. The scale bars represent 50 μm.

Comparison of the MeOB6OABX and MeOBO5OABX dimers
Comparing the melting points of the MeOB6OABX dimers with those of the MeOBO5OABX dimers reveals an increase on replacing a methylene-link by an

ether-link ranging from 31.7°C for X=BuO to 41°C for X=Et. These increases presumably reflect the more linear shape of the MeOBO5OABX dimers allowing for a greater packing efficiency in the crystal phase coupled with stronger intermolecular interactions arising from the ether-link.

The values of T_{NI} for the MeOBO5OABX dimers are also higher than the MeOB6OABX dimers. The differences range fom 30.4°C for X=BuO to 38.3°C for X=Et. These are typical values observed for the change in T_{NI} on replacing a methylene-link by an ether-link in similar materials [64]. The nematic-isotropic entropy changes ($\Delta S_{NI}/R$) are also higher for the MeOBO5OABX dimers than for the MeOB6OABX dimers. These increases in both T_{NI} and $\Delta S_{NI}/R$ on replacing a methylene- by an ether-link in odd-membered liquid crystal dimes are wholly consistent with the predictions of the theoretical model developed by Luckhurst and coworkers referred to earlier [82-84]. The difference in molecular curvature between corresponding MeOB6OABX and MeOBO5OABX dimers arising from the larger bond angle associated with an ether-link compared to a methylene-link is immediately apparent in Figure 7 which shows space filling models of MeOB6OABCN and MeOBO5OABCN in the all-*trans* conformation. We should note that, as for other structurally similar dimers [29, 36, 38, 64], in the calculated ground state of these dimers in vacuo, the O-C-C-C dihedral adopts a gauche conformation. However, the energy difference between the calculated ground state and all-*trans* conformation is small, of the order of 1 kJ mol^{-1}, and presumably will be very different in an ordered liquid crystal environment which will preferentially select more linear conformations [87]. For this reason we consider the all-*trans* conformation a better representation of the average molecular shape when discussing the transitional behaviour of these and similar dimers.
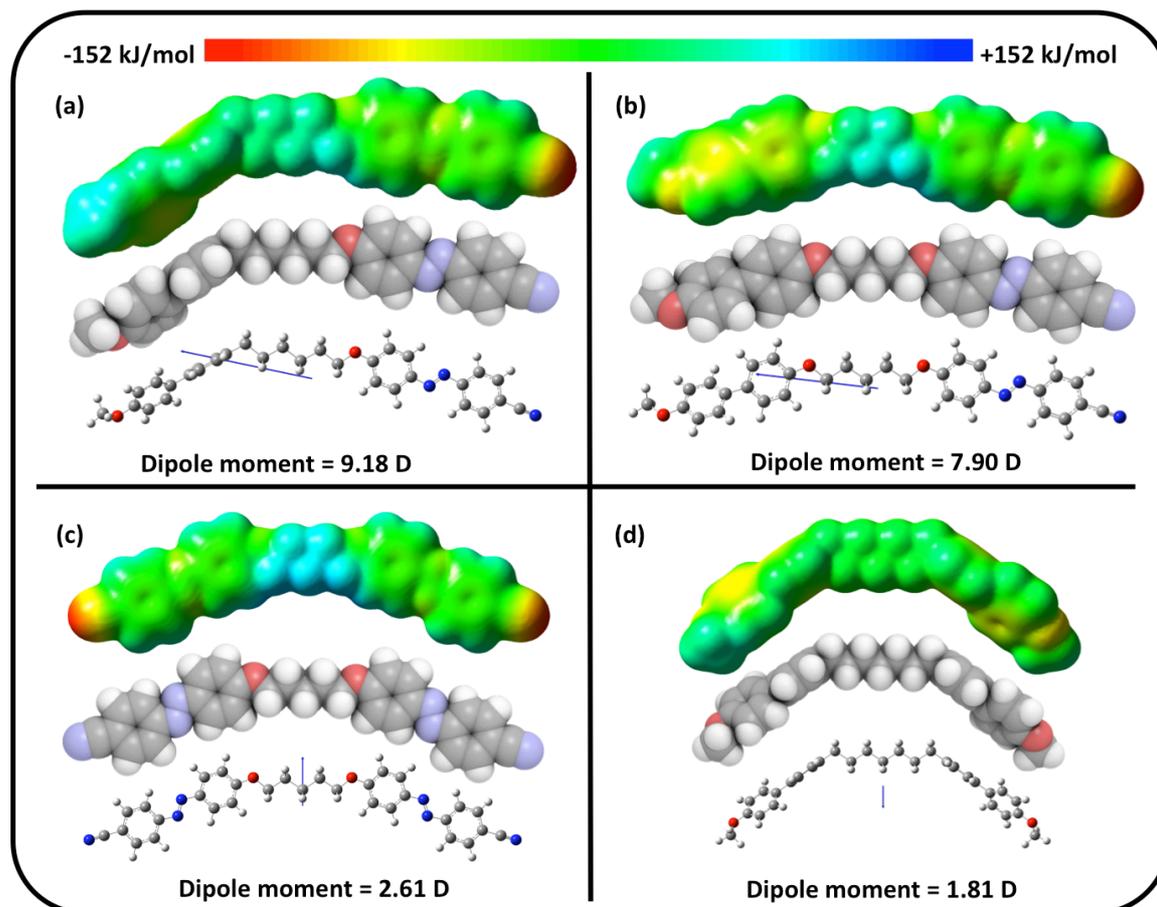
Figure 7. The electrostatic potential isosurfaces with an isovalue of 0.0004 (top), space filling (middle) and ball-and-stick models showing the molecular dipole moment (bottom) for the all *trans* conformations of (a) MeOB6OABCN, (b) MeOBO5OABCN, (c) CNABO5OABCN and (d)MeOB7BOMe. The lengths of the arrows indicating the dipole moments are not to scale.

We now turn our attention to the differences observed within each series on varying the terminal group. For the MeOB6OABX dimers the efficiency of the terminal group X in promoting T_{NI} is:

CN > OMe > OBu > Me > Et > Bu

and the same order was found for the CB6OABX dimers [64]. The corresponding order for the MeOBO5OABX dimers is identical and observed also for the CBO5OABX dimers [64]. This order for all four sets of dimers may be accounted for in terms of the changes in the average molecular shape [88-90] and the

strength of the mixed mesogen interaction [19, 91, 92] on varying X. We have shown previously that there is no simple relationship between the electronic distribution within the OABX mesogenic units in non-symmetric dimers and T_{NI} [64].

The nematic-isotropic transition temperatures of the non-symmetric dimers may be compared to the average of those of the parent symmetric dimers in order to assess the importance of the mixed mesogenic unit interaction in determining their phase behaviour. This comparison is normally expressed in terms of a scaled deviation, ΔT_{SC}, given by [17]:

$$\Delta T_{SC} = \frac{2T_{AB} - (T_A + T_B)}{T_A + T_B} \qquad (1)$$

where T_{AB} is the T_{NI} of the non-symmetric dimer, and T_A and T_B those of the corresponding symmetric dimers. The transitional properties of the XABO5OABX dimers have been reported elsewhere [64] with the exception of EtABO5OABEt which exhibits a monotropic nematic phase assigned on the basis of the observation of a characteristic Schlieren nematic texture; the associated transitional properties are:

Cr 166.8°C (ΔH_{CrI}=57.44 kJ mol^{-1}) N 146.1°C (ΔH_{NI}=1.21 kJ mol^{-1}; $\Delta S_{NI}/R$=0.35) I.

To calculate ΔT_{SC} for the MeOB6OABX and MeOBO5OABX dimers, we also require the transition temperatures of MeOB7BOMe and MeOBO5OBOMe, respectively. MeOB7BOMe melts directly into the isotropic phase at 154.1°C. The isotropic liquid may be supercooled to 120°C prior to crystallisation but without the observation of liquid crystallinity. MeOB7BOMe is only poorly soluble and it was not possible to construct a binary phase diagram with CB7CB in order to obtain virtual transition temperatures. However, we succeeded in preparing a homogeneous approximately equimolar mixture of the two components and this showed a N_{TB}-N transition at 93.9°C and T_{NI} at 106.0°C. The N and N_{TB} phases were assigned on the basis of the optical textures observed for isolated droplets, see Figure 8. If we assume a linear dependence of both $T_{N_{TB}N}$ and T_{NI} on composition then the extrapolated values of $T_{N_{TB}N}$ and T_{NI} for MeOB7BOMe are 86°C and 97°C, respectively. It may normally be considered unwise to extrapolate

virtual transition temperatures using data for just a single mixture but we note that the temperatures obtained in this case closely follow the trends in behaviour observed for structurally similar materials on exchanging cyano and methoxy groups [38]. Specifically, on passing from CB7CB to MeOB7BOMe we see reductions in both $T_{N_{TB}N}$ and T_{NI} of 17.6°C and 19.1°C, respectively, and on changing CB6OCB to MeOB6OBOMe the reductions are 10°C and 22°C, respectively.
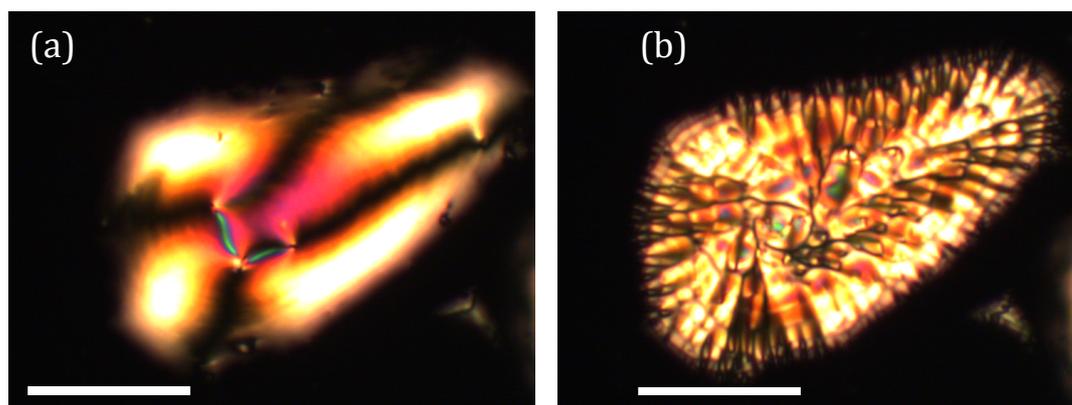

Figure 8. (a) The nematic Schlieren texture (T=100°C) and (b) the polygonal texture of the twist-bend nematic phase (T=93°C) shown by a binary mixture of MeOB7BOMe and CB7CB containing 52 mol% MeOB7BOMe. Images represent the same approximate region. Scale bar represents 50 μm.

MeOBO5OBOMe also melts directly into the isotropic phase at 208.7°C. Isolated droplets of the isotropic liquid can be supercooled to 130°C prior to crystallisation and without the observation of liquid crystalline behaviour. MeOBO5OBOMe is a very insoluble material and it was not possible to prepare homogeneous mixtures of this with CB7CB in order to estimate a virtual T_{NI}. The discussion of the scaled deviations, ΔT_{SC}, is restricted therefore to those of the MeOB6OABX dimers and these are listed in Table 3. Negative values of ΔT_{SC} are observed for these dimers with the exception of MeOB6OABOMe for which a positive value is seen. This behaviour contrasts with that seen for the CB6OABX dimers for which a negative value of ΔT_{SC} is seen only for CB6OABBu, see Table 3. The value of ΔT_{SC} for the MeOB6OABX dimers decreases in the order:

$$OMe > OBu > CN > Me > Et > Bu$$

and this trend is similar to that seen for T_{NI} with the exception of MeOB6OABCN which shows the highest value of T_{NI}. This trend in ΔT_{SC} is also similar to that seen for the CB6OABX dimers except the positions of OBu and CN are inverted.

Table 3. The values of ΔT_{SC}, defined in equation 1, and expressed as a percentage for the MeOB6OABX dimers. Also listed are the ΔT_{SC} values for the CB6OABX dimers taken from [64].

X	MeOB6OABX ΔT_{SC} / %	CB6OABX ΔT_{SC} / %
Me	-1.98	0
MeO	0.86	1.86
Et	-2.40	*-
Bu	-2.80	-1.12
BuO	-0.29	0.59
CN	-1.50	1.56
NO$_2$	*-	1.56

* Dimers not prepared.

The values of ΔT_{SC} may be interpreted within the framework of the molecular field theory developed to predict phase diagrams for binary mixtures of nematics and referred to earlier [81]. This model considers three intermolecular interaction parameters; specifically, two between like species, ε_{AA} and ε_{BB}, and one representing the interaction between the unlike mesogens, ε_{AB}. The model predicts that when ε_{AB} is the geometric mean of ε_{AA} and ε_{BB} then the transition temperatures of the binary mixtures are simply the weighted averages of those of the pure components, and a linear dependence of T_{NI} on composition is observed giving ΔT_{SC}=0. Such behaviour is described as being ideal and deviations from it are observed when ε_{AB} is allowed to deviate from being the geometric mean of ε_{AA} and ε_{BB}. If ε_{AB} is greater than the geometric mean of ε_{AA} and ε_{BB}, then the T_{NI} line is curved and lies above the straight line representing

ideal behaviour and $\Delta T_{SC}>0$. Conversely, a negative deviation in ε_{AB} gives a curved T_{NI} line lying below the ideal line and $\Delta T_{SC}<0$. Even small deviations in ε_{AB} of 1.85% give rise to a curved N-I phase boundary on the phase diagram.

Returning to the values of ΔT_{SC} listed in Table 3 for the MeOB6OABX dimers, we note that these are all relatively small. The negative values may be accounted for in terms of the mixed mesogen interaction being less favourable than the geometric mean of the interactions between the like mesogens, and mixing is presumably entropically driven. The small and positive ΔT_{SC} for MeOB6OABOMe may arise from a combination of a favourable interaction between the ether units and steric compatibility of the terminal groups. Indeed, it is noteworthy that MeOB6OABOMe exhibits the highest melting point of this set of materials. It may appear surprising that MeOB6OABCN exhibits a higher T_{NI} than MeOB6OABOMe given their respective values of ΔT_{SC} but this suggests that the formation of antiparallel associated pairs of MeOB6OABCN molecules serve to enhance shape anisotropy increasing T_{NI}. Similar behaviour was observed for the CB6OABX dimers [64].

It is striking that the ΔT_{SC} values tend to be negative for the MeOB6OABX dimers and positive for the CB6OABX dimers, see Table 3. Non-symmetric dimers containing electron rich and deficient mesogenic moieties have a tendency to show intercalated smectic phases[18]. The driving force for the formation of these phases is considered to be a favourable mixed core interaction and it has been suggested that this may be an electrostatic quadrupolar interaction between groups with quadrupole moments which are opposite in sign [93]. Presumably it is this interaction that gives rise to the positive values of ΔT_{SC} seen for the CB6OABX dimers.

We now turn our attention to the role of X in promoting the N_{TB} phase for the MeOB6OABX dimers. The efficiency of the terminal group X in enhancing $T_{N_{TB}N}$ is:

$$CN > OMe > OBu > Me > Bu > Et.$$

This is the same trend as observed for T_{NI} with the exception of the reversal of Bu and Et. This may reflect the ability of Bu to pack more efficiently into the locally intercalated arrangement of the molecules commonly observed for the N_{TB} phase [36]. The spread of T_{NI} for the MeOB6OABX dimers is 50.9°C whereas

of $T_{N_{TB}N}$ is 40.8°C. This suggests that the overall molecular curvature arising primarily from the hexyloxy spacer has a larger effect in determining $T_{N_{TB}N}$ whereas the terminal group, X, has a greater influence on T_{NI}. Similar behaviour was observed for the CB6OABX dimers [64]. For the MeOBO5OABX dimers only MeOBO5OABCN exhibited the N_{TB} phase, and $T_{N_{TB}N}$ is 16.1°C lower than that for MeOB6OABCB. This reduction is consistent with that seen for the CB6OABX and CBO5OABX dimers [64]. The absence of N_{TB} behaviour for the remaining MeOBO5OABX dimers presumably reflects the lowest temperatures to which these materials could be supercooled prior to crystallisation.

If we now compare T_{NI} for the MeOB6OABX dimers with those of the corresponding CB6OABX dimers, the value for the latter is always greater, and difference decreases in the order:

$$CN > Me > Bu > OMe > OBu .$$
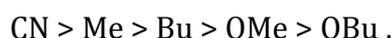
This is consistent with the higher ΔT_{SC} values for the CB6OABX dimers (Table 3) suggesting a favourable specific interaction between the unlike mesogenic units, although the spread of these differences is rather small. For X=CN T_{NI} is 22.1°C higher for CB6OABCN than MeOB6OABCN, and for X=OBu the difference is 12.2°C. The same trend is seen on comparing the T_{NI} values for the MeOBO5OABX and CBO5OABX dimers, although the range of differences is slightly smaller: 19.6°C for X=CN to 10.6°C for X=OBu, and for any given X, the difference is smaller. This suggests that the effect X has on the shape anisotropy of the molecule is smaller for the more linear ether-linked dimers.

The values of $T_{N_{TB}N}$ are also consistently higher for the CB6OABX dimers, although the order in which the difference decreases differs from that seen for T_{NI}:

$$Me > CN > OBu > Bu > OMe.$$

This reinforces the observation that terminal substituents appear to influence $T_{N_{TB}N}$ and T_{NI} differently. The spread of the differences between the corresponding members of each set of materials is about the same but the absolute differences are smaller ranging from 17.6°C (X=Me) to 6.1°C (X=OMe). It is noteworthy that the values of $T_{N_{TB}N}$ are higher for the CB6OABX dimers although the shapes of the two sets of dimers are very similar. This indicates that

although a bent shape is required for the observation of the N_{TB} phase other factors such as the interaction strength parameters between the mesogenic units must also be taken into account.

References

[1]   Tschierske C. Mirror symmetry breaking in liquids and liquid crystals. Liq Cryst. 2018;45(13-15):2221-2252.

[2]   Meyer R.B. In Balian RG, Weil G, Eds. *Les Houches summer school in theoretical physics*; New York (NY): Gordon and Breach; 1976. p. 273-373.

[3]   Dozov I. On the spontaneous symmetry breaking in the mesophases of achiral banana-shaped molecules. Europhys Lett. 2001;56(2):247-253.

[4]   Cestari M, Diez-Berart S, Dunmur DA, Ferrarini A, de la Fuente MR, Jackson DJB, Lopez DO, Luckhurst GR, Perez-Jubindo MA, Richardson RM, Salud J, Timimi BA, Zimmermann H. Phase behavior and properties of the liquid-crystal dimer 1 '',7 ''-bis(4-cyanobiphenyl-4 '- yl) heptane: A twist-bend nematic liquid crystal. Phys Rev E. 2011;84(3):031704.

[5]   Borshch V, Kim YK, Xiang J, Gao M, Jakli A, Panov VP, Vij JK, Imrie CT, Tamba MG, Mehl GH, Lavrentovich OD. Nematic twist-bend phase with nanoscale modulation of molecular orientation. Nat Commun. 2013;4:2635.

[6]   Chen D, Porada JH, Hooper JB, Klittnick A, Shen YQ, Tuchband MR, Korblova E, Bedrov D, Walba DM, Glaser MA, Maclennan JE, Clark NA. Chiral heliconical ground state of nanoscale pitch in a nematic liquid crystal of achiral molecular dimers. Proc Nat Acad Sci USA. 2013;110(40):15931-15936.

[7]   Zhu CH, Tuchband MR, Young A, Shuai M, Scarbrough A, Walba DM, Maclennan JE, Wang C, Hexemer A, Clark NA. Resonant Carbon K-Edge Soft X-Ray Scattering from Lattice-Free Heliconical Molecular Ordering: Soft Dilative Elasticity of the Twist-Bend Liquid Crystal Phase. Phys Rev Lett. 2016;116(14):147803.

[8]   Sepelj M, Lesac A, Baumeister U, Diele S, Nguyen HL, Bruce DW. Intercalated liquid-crystalline phases formed by symmetric dimers with an alpha,omega-diiminoalkylene spacer. J Mater Chem. 2007;17(12):1154-1165.

[9]   Panov VP, Nagaraj M, Vij JK, Panarin YP, Kohlmeier A, Tamba MG, Lewis RA, Mehl GH. Spontaneous Periodic Deformations in Nonchiral Planar-Aligned Bimesogens with a Nematic-Nematic Transition and a Negative Elastic Constant. Phys Rev Lett. 2010;105(16):167801.

[10]   Abberley JP, Killah R, Walker R, Storey JMD, Imrie CT, Salamonczyk M, Zhu CH, Gorecka E, Pociecha D. Heliconical smectic phases formed by achiral molecules. Nat Commun. 2018;9:228.

[11]   Salamonczyk M, Vaupotic N, Pociecha D, Walker R, Storey JMD, Imrie CT, Wang C, Zhu CH, Gorecka E. Multi-level chirality in liquid crystals formed by achiral molecules. Nature Commun. 2019;10:1922.

[12]   Imrie CT, Henderson PA. Liquid crystal dimers and oligomers. Curr Opin Colloid Interface Sci. 2002;7(5-6):298-311.

[13]   Imrie CT, Henderson PA. Liquid crystal dimers and higher oligomers: Between monomers and polymers. Chem Soc Rev. 2007;36(12):2096-2124.

[14]   Luckhurst GR. Liquid-crystal dimers and oligomers - experiment and theory. Macromolecular Symp. 1995;96:1-26.

[15]   Imrie CT, Karasz FE, Attard GS. Comparison of the mesogenic properties of monomeric, dimeric, and side-chain polymeric liquid-crystals. Macromolecules. 1993;26(3):545-550.

[16]   Hogan JL, Imrie CT, Luckhurst GR. Asymmetric dimeric liquid-crystals - the preparation and properties of the alpha-(4-cyanobiphenyl-4'-oxy)-omega-(4-normal-alkylanilinebenzylidene-4 '-oxy)hexanes. Liq Cryst. 1988;3(5):645-650.

[17]   Attard GS, Date RW, Imrie CT, Luckhurst GR, Roskilly SJ, Seddon JM, Taylor L. Nonsymmetrical dimeric liquid-crystals - the preparation and properties of the alpha-(4-cyanobiphenyl-4'-yloxy)-omega-(4-n-alkylanilinebenzylidene-4'-o xy)alkanes. Liq Cryst. 1994;16(4):529-581.

[18]   Imrie CT. Non-symmetric liquid crystal dimers: How to make molecules intercalate. Liq Cryst. 2006;33(11-12):1449-1454.

[19]   Yeap G-Y, Hng T-C, Yeap S-Y, Gorecka E, Ito MM, Ueno K, Okamoto M, Mahmood WAK, Imrie CT. Why do non-symmetric dimers intercalate? The synthesis and characterisation of the -(4-benzylidene-substituted-aniline-4'-oxy)--(2-methylbutyl-4'-(4''-phen yl)benzoateoxy)alkanes. Liq Cryst. 2009;36(12):1431-1441.

[20]   Henderson PA, Niemeyer O, Imrie CT. Methylene-linked liquid crystal dimers. Liq Cryst. 2001;28(3):463-472.

[21]   Henderson PA, Seddon JM, Imrie CT. Methylene- and ether-linked liquid crystal dimers II. Effects of mesogenic linking unit and terminal chain length. Liq Cryst. 2005;32(11-12):1499-1513.

[22]   Henderson PA, Imrie CT. Methylene-linked liquid crystal dimers and the twist-bend nematic phase. Liq Cryst. 2011;38(11-12):1407-1414.

[23]   Mandle RJ, Goodby JW. Does Topology Dictate the Incidence of the Twist-Bend Phase? Insights Gained from Novel Unsymmetrical Bimesogens. Chem Eur J. 2016;22(51):18456-18464.

[24]   Mandle RJ, Goodby JW. Dependence of Mesomorphic Behaviour of Methylene-Linked Dimers and the Stability of the N-TB/N-X Phase upon Choice of Mesogenic Units and Terminal Chain Length. Chem Eur J. 2016;22(27):9366-9374.

[25]   Panov VP, Vij JK, Mehl GH. Twist-bend nematic phase in cyanobiphenyls and difluoroterphenyls bimesogens. Liq Cryst. 2017;44(1):147-159.

[26]   Ahmed Z, Welch C, Mehl GH. The design and investigation of the self-assembly of dimers with two nematic phases. RSC Adv. 2015;5(113):93513-93521.

[27]   Stevenson WD, Zou HX, Zeng XB, Welch C, Ungar G, Mehl GH. Dynamic calorimetry and XRD studies of the nematic and twist-bend nematic phase transitions in a series of dimers with increasing spacer length. Phys Chem Chem Phys. 2018;20(39):25268-25274.

[28]   Ramou E, Welch C, Hussey J, Ahmed Z, Karahaliou PK, Mehl GH. The induction of the N-tb phase in mixtures. Liq Cryst. 2018;45(13-15):1929-1935.

[29]   Paterson DA, Gao M, Kim YK, Jamali A, Finley KL, Robles-Hernandez B, Diez-Berart S, Salud J, de la Fuente MR, Timimi BA, Zimmermann H, Greco C, Ferrarini A, Storey JMD, Lopez DO, Lavrentovich OD, Luckhurst GR, Imrie CT. Understanding the twist-bend nematic phase: the characterisation of 1-(4-cyanobiphenyl-4 '-yloxy)-6-(4-cyanobiphenyl-4 '-yl)hexane (CB6OCB) and comparison with CB7CB. Soft Matter. 2016;12(32):6827-6840.

[30]   Sebastian N, Lopez DO, Robles-Hernandez B, de la Fuente MR, Salud J, Perez-Jubindo MA, Dunmur DA, Luckhurst GR, Jackson DJB. Dielectric, calorimetric and mesophase properties of 1 ''-(2 ',4-difluorobiphenyl-4 '-yloxy)-9 ''-(4-cyano-biphenyl-4 '-yloxy) nonane: an odd liquid crystal dimer with a monotropic mesophase having the characteristics of a twist-bend nematic phase. Phys Chem Chem Phys. 2014;16(39):21391-21406.

[31]   Lu ZB, Henderson PA, Paterson BJA, Imrie CT. Liquid crystal dimers and the twist-bend nematic phase. The preparation and characterisation of the alpha,omega-bis(4-cyanobiphenyl-4 '-yl) alkanedioates. Liq Cryst. 2014;41(3):471-483.

[32]   Mandle RJ, Voll CCA, Lewis DJ, Goodby JW. Etheric bimesogens and the twist-bend nematic phase. Liq Cryst. 2016;43(1):13-21.

[33]   Ivsic T, Baumeister U, Dokli I, Mikleusevic A, Lesac A. Sensitivity of the N-TB phase formation to the molecular structure of imino-linked dimers. Liq Cryst. 2017;44(1):93-105.

[34]   Dawood AA, Grossel MC, Luckhurst GR, Richardson RM, Timimi BA, Wells NJ, Yousif YZ. On the twist-bend nematic phase formed directly from the isotropic phase. Liq Cryst. 2016;43(1):2-12.

[35]   Dawood AA, Grossel MC, Luckhurst GR, Richardson RM, Timimi BA, Wells NJ, Yousif YZ. Twist-bend nematics, liquid crystal dimers, structure-property relations. Liq Cryst. 2017;44(1):106-126.

[36]   Paterson DA, Abberley JP, Harrison WT, Storey JM, Imrie CT. Cyanobiphenyl-based liquid crystal dimers and the twist-bend nematic phase. Liq Cryst. 2017;44(1):127-146.

[37]   Archbold CT, Andrews JL, Mandle RJ, Cowling SJ, Goodby JW. Effect of the linking unit on the twist-bend nematic phase in liquid crystal dimers: a comparative study of two homologous series of methylene- and ether-linked dimers. Liq Cryst. 2017;44(1):84-92.

[38]   Abberley JP, Jansze SM, Walker R, Paterson DA, Henderson PA, Marcelis ATM, Storey JMD, Imrie CT. Structure-property relationships in twist-bend nematogens: the influence of terminal groups. Liq Cryst. 2017;44(1):68-83.

[39]   Mandle RJ, Stevens MP, Goodby JW. Developments in liquid-crystalline dimers and oligomers. Liq Cryst. 2017;44(12-13):2046-2059.

[40]   Paterson DA, Crawford CA, Pociecha D, Walker R, Storey JMD, Gorecka E, Imrie CT. The role of a terminal chain in promoting the twist-bend nematic phase: the synthesis and characterisation of the 1-(4-cyanobiphenyl-4 '-yl)-6-(4-alkyloxyanilinebenzylidene-4 '-oxy)hexanes. Liq Cryst. 2018;45(13-15):2341-2351.

[41]   Lesac A, Baumeister U, Dokli I, Hamersak Z, Ivsic T, Kontrec D, Viskic M, Knezevic A, Mandle RJ. Geometric aspects influencing N-N-TB transition - implication of intramolecular torsion. Liq Cryst. 2018;45(7):1101-1110.

[42] Watanabe K, Tamura T, Kang SM, Tokita M. Twist bend nematic liquid crystals prepared by one-step condensation of 4-(4-Pentylcyclohexyl) benzoic acid and alkyl diol. Liq Cryst. 2018;45(6):924-930.

[43] Chen D, Nakata M, Shao RF, Tuchband MR, Shuai M, Baumeister U, Weissflog W, Walba DM, Glaser MA, Maclennan JE, Clark NA. Twist-bend heliconical chiral nematic liquid crystal phase of an achiral rigid bent-core mesogen. Phys Rev E. 2014;89(2):022506.

[44] Sreenilayam SP, Panov VP, Vij JK, Shanker G. The N-TB phase in an achiral asymmetrical bent-core liquid crystal terminated with symmetric alkyl chains. Liq Cryst. 2017;44(1):244-253.

[45] Mandle RJ, Goodby JW. Progression from nano to macro science in soft matter systems: dimers to trimers and oligomers in twist-bend liquid crystals. RSC Adv. 2016;6(41):34885-34893.

[46] Wang Y, Singh G, Agra-Kooijman DM, Gao M, Bisoyi HK, Xue CM, Fisch MR, Kumar S, Li Q. Room temperature heliconical twist-bend nematic liquid crystal. Crystengcomm. 2015;17(14):2778-2782.

[47] Simpson FP, Mandle RJ, Moore JN, Goodby JW. Investigating the Cusp between the nano-and macro-sciences in supermolecular liquid-crystalline twist-bend nematogens. J Mater Chem C. 2017;5(21):5102-5110.

[48] Al-Janabi A, Mandle RJ, Goodby JW. Isomeric trimesogens exhibiting modulated nematic mesophases. RSC Adv. 2017;7(75):47235-47242.

[49] Tuchband MR, Paterson DA, Salamonczyk M, Norman VA, Scarbrough AN, Forsyth E, Garcia E, Wang C, Storey JMD, Walba DM, Sprunt S, Jakli A, Zhu C, Imrie CT, Clark NA. Distinct differences in the nanoscale behaviors of the twist–bend liquid crystal phase of a flexible linear trimer and homologous dimer. Proc Nat Acad Sci USA. 2019:DOI: 10.1073/pnas.1821372116.

[50] Jansze SM, Martinez-Felipe A, Storey JMD, Marcelis ATM, Imrie CT. A Twist-Bend Nematic Phase Driven by Hydrogen Bonding. Angew Chem Int Ed. 2015;54(2):643-646.

[51] Paterson DA, Martinez-Felipe A, Jansze SM, Marcelis ATM, Storey JMD, Imrie CT. New insights into the liquid crystal behaviour of hydrogen-bonded mixtures provided by temperature-dependent FTIR spectroscopy. Liq Cryst. 2015;42(5-6):928-939.

[52] Walker R, Pociecha D, Abberley JP, Martinez-Felipe A, Paterson DA, Forsyth E, Lawrence GB, Henderson PA, Storey JMD, Gorecka E, Imrie CT. Spontaneous chirality through mixing achiral components: a twist-bend nematic phase driven by hydrogen-bonding between unlike components. Chem Commun. 2018;54(27):3383-3386.

[53] Greco C, Luckhurst GR, Ferrarini A. Molecular geometry, twist-bend nematic phase and unconventional elasticity: a generalised Maier-Saupe theory. Soft Matter. 2014;10(46):9318-9323.

[54] Archbold CT, Mandle RJ, Andrews JL, Cowling SJ, Goodby JW. Conformational landscapes of bimesogenic compounds and their implications for the formation of modulated nematic phases. Liq Cryst. 2017;44(12-13):2079-2088.

[55] Walker R, Pociecha D, Strachan GJ, Storey JMD, Gorecka E, Imrie CT. Molecular curvature, specific intermolecular interactions and the twist

bend nematic phase: the synthesis and characterisation of the 1-(4-cyanobiphenyl-4′-yl)-6-(4-alkylanilinebenzylidene-4′-oxy)hexanes (CB6O.m). Soft Matter. 2019:3188-3197.

[56] Pocock EE, Mandle RJ, Goodby JW. Molecular shape as a means to control the incidence of the nanostructured twist bend phase. Soft Matter. 2018;14(13):2508-2514.

[57] Adlem K, Copic M, Luckhurst GR, Mertelj A, Parri O, Richardson RM, Snow BD, Timimi BA, Tuffin RP, Wilkes D. Chemically induced twist-bend nematic liquid crystals, liquid crystal dimers, and negative elastic constants. Phys Rev E. 2013;88(2):022503.

[58] Cestari M, Frezza E, Ferrarini A, Luckhurst GR. Crucial role of molecular curvature for the bend elastic and flexoelectric properties of liquid crystals: mesogenic dimers as a case study. J Mater Chem. 2011;21(33):12303-12308.

[59] Xiang J, Li YN, Li Q, Paterson DA, Storey JMD, Imrie CT, Lavrentovich OD. Electrically Tunable Selective Reflection of Light from Ultraviolet to Visible and Infrared by Heliconical Cholesterics. Adv Mater. 2015;27(19):3014-3018.

[60] Salili SM, Xiang J, Wang H, Li Q, Paterson DA, Storey JMD, Imrie CT, Lavrentovich OD, Sprunt SN, Gleeson JT, Jakli A. Magnetically tunable selective reflection of light by heliconical cholesterics. Phys Rev E. 2016;94(4):042705.

[61] Xiang J, Varanytsia A, Minkowski F, Paterson DA, Storey JMD, Imrie CT, Lavrentovich OD, Palffy-Muhoray P. Electrically tunable laser based on oblique heliconical cholesteric liquid crystal. Proc Nat Acad Sci USA. 2016;113(46):12925-12928.

[62] Joshi V, Paterson DA, Storey JMD, Imrie CT, Chien LC. Tunable backflow in chiral nematic liquid crystals via twist-bend nematogens and surface-localised &ITin&IT-&ITsitu &ITpolymer protrusions. Liq Cryst. 2017;44(14-15):2327-2336.

[63] Archbold CT, Davis EJ, Mandle RJ, Cowling SJ, Goodby JW. Chiral dopants and the twist-bend nematic phase - induction of novel mesomorphic behaviour in an apolar bimesogen. Soft Matter. 2015;11(38):7547-7557.

[64] Paterson DA, Walker R, Abberley JP, Forestier J, Harrison WTA, Storey JMD, Pociecha D, Gorecka E, Imrie CT. Azobenzene-based liquid crystal dimers and the twist-bend nematic phase. Liq Cryst. 2017;44(12-13):2060-2078.

[65] Eremin A, Nadasi H, Hirankittiwong P, Kiang-Ia J, Chattham N, Haba O, Yonetake K, Takezoe H. Azodendrimers as a photoactive interface for liquid crystals. Liq Cryst. 2018;45(13-15):2121-2131.

[66] Palermo G, Guglielmelli A, Pezzi L, Cataldi U, De Sio L, Caputo R, De Luca A, Burgi T, Tabiryan N, Umeton C. A command layer for anisotropic plasmonic photo-thermal effects in liquid crystal. Liq Cryst. 2018;45(13-15):2214-2220.

[67] Ube T, Yoda T, Ikeda T. Fabrication of photomobile polymer materials with phase-separated structure of crosslinked azobenzene liquid-crystalline polymer and poly(dimethylsiloxane). Liq Cryst. 2018;45(13-15):2269-2273.

[68] Goda K, Omori M, Takatoh K. Optical switching in guest-host liquid crystal devices driven by photo- and thermal isomerisation of azobenzene. Liq Cryst. 2018;45(4):485-490.

[69] Paterson DA, Xiang J, Singh G, Walker R, Agra-Kooijman DM, Martinez-Felipe A, Gan M, Storey JMD, Kumar S, Lavrentovich OD, Imrie CT. Reversible Isothermal Twist-Bend Nematic-Nematic Phase Transition Driven by the Photoisomerization of an Azobenzene-Based Nonsymmetric Liquid Crystal Dinner. J Am Chem Soc. 2016;138(16):5283-5289.

[70] Yoshioka J, Salamon P, Paterson DA, Storey JMD, Imrie CT, Jakli A, Araoka F, Buka A. Spherical-cap droplets of a photo-responsive bent liquid crystal dimer. Soft Matter. 2019;15(5):989-998.

[71] Aya S, Salamon P, Paterson DA, Storey JMD, Imrie CT, Araoka F, Jakli A, Buka A. Fast-and-Giant Photorheological Effect in a Liquid Crystal Dimer. Adv Mater Interfaces. 2019;6:1802032.

[72] Craig AA, Imrie CT. Effect of spacer length on the thermal-properties of side-chain liquid-crystal poly(methacrylate)s. J Mater Chem. 1994;4(11):1705-1714.

[73] Blatch AE, Luckhurst GR. The liquid crystal properties of symmetric and non-symmetric dimers based on the azobenzene mesogenic group. Liq Cryst. 2000;27(6):775-787.

[74] Imrie CT, Karasz FE, Attard GS. Side-chain liquid-crystalline copolymers .2. polystyrene-based side-chain polymers containing nitroazobenzene. Macromolecules. 1994;27(6):1578-1581.

[75] Imrie CT, Schleeh T, Karasz FE, Attard GS. Dependence of the transitional properties of polystyrene-based side-chain liquid-crystalline polymers on the chemical nature of the mesogenic group. Macromolecules. 1993;26(3):539-544.

[76] Imrie CT, Karasz FE, Attard GS. Side-chain liquid-crystalline copolymers containing charge-transfer groups. Liq Cryst. 1991;9(1):47-57.

[77] Stewart D, Imrie CT. Synthesis and characterization of spin-labelled and spin-probed side-chain liquid crystal polymers. Polymer. 1996;37(15):3419-3425.

[78] Frisch MJ, et al Gaussian 09 (Revision B.01). Wallingford CT: Gaussian Inc.; 2010.

[79] Tarini M, Cignoni P, Montani C. Ambient Occlusion and Edge Cueing for Enhancing Real Time Molecular Visualization IEEE Trans Visualization and Computer Graphics. 2006;12(5):1237-1244.

[80] Dennington R, Keith T, Millam J. Gauss View, Version 5. Shawnee Mission, KS: Semichem Inc; 2009.

[81] Humphries R, James P, Luckhurst GR. A molecular field treatment of liquid crystalline mixtures. Symp Faraday Soc. 1971;5:107-118.

[82] Emerson APJ, Luckhurst GR. On the relative propensities of ether and methylene linkages for liquid-crystal formation in calamitics. Liq Cryst. 1991;10(6):861-868.

[83] Ferrarini A, Luckhurst GR, Nordio PL, Roskilly SJ. Prediction of the transitional properties of liquid-crystal dimers - a molecular-field calculation based on the surface tensor parametrization. J Chem Phys. 1994;100(2):1460-1469.

[84]   Ferrarini A, Luckhurst GR, Nordio PL, Roskilly SJ. Understanding the dependence of the transitional properties of liquid crystal dimers on their molecular geometry. Liq Cryst. 1996;21(3):373-382.

[85]   Date RW, Imrie CT, Luckhurst GR, Seddon JM. Smectogenic dimeric liquid-crystals - the preparation and properties of the α,ω-bis(4-normal-alkylanilinebenzylidine-4'-oxy)alkanes. Liq Cryst. 1992;12(2):203-238.

[86]   Henderson PA, Cook AG, Imrie CT. Oligomeric liquid crystals: From monomers to trimers. Liq Cryst. 2004;31(11):1427-1434.

[87]   Emsley JW, De Luca G, Lesage A, Merlet D, Pileio G. The structure and conformation of a mesogenic compound between almost zero and almost complete orientational order. Liq Cryst. 2007;34(9):1071-1093.

[88]   Yeap GY, Osman F, Imrie CT. Non-symmetric dimers: effects of varying the mesogenic linking unit and terminal substituent. Liq Cryst. 2015;42(4):543-554.

[89]   Yeap GY, Lee HC, Mahmood WAK, Imrie CT, Takeuchi D, Osakada K. Synthesis, thermal and optical behaviour of non-symmetric liquid crystal dimers alpha-(4-benzylidene-substituted-aniline-4 '-oxy)-omega- pentyl-4-(4 '-phenyl)benzoateoxy hexane. Phase Trans. 2011;84(1):29-37.

[90]   Goodby JW. Free volume, molecular grains, self-organisation, and anisotropic entropy: machining materials. Liq Cryst. 2017;44(12-13):1755-1763.

[91]   Attard GS, Garnett S, Hickman CG, Imrie CT, Taylor L. Asymmetric dimeric liquid-crystals with charge-transfer groups. Liq Cryst. 1990;7(4):495-508.

[92]   Schleeh T, Imrie CT, Rice DM, Karasz FE, Attard GS. Ultrastructure studies of polystyrene-based side-chain liquid-crystalline copolymers containing charge-transfer groups. J Polym Sci Part a-Polym Chem. 1993;31(7):1859-1869.

[93]   Blatch AE, Fletcher ID, Luckhurst GR. The intercalated smectic-a phase - the liquid-crystal properties of the α-(4-cyanobiphenyl-4'-yloxy)-ω-(4-alkyloxycinnamoate)alkanes. Liq Cryst. 1995;18(5):801-809.